

## Magnetic signatures of ferromagnetic polarons in $\text{La}_{0.7}\text{Ca}_{0.3}\text{MnO}_3$ : Colossal magnetoresistance is not a Griffiths singularity

J. A. Souza,<sup>1,\*</sup> J. J. Neumeier,<sup>1</sup> and Yi-Kuo Yu<sup>2</sup>

<sup>1</sup>*Department of Physics, P.O. Box 173840, Montana State University, Bozeman, Montana 59717-3840, USA*

<sup>2</sup>*National Center for Biotechnology Information, 8600 Rockville Pike, Bethesda, Maryland 20894, USA*

(Received 29 October 2007; revised manuscript received 30 May 2008; published 31 July 2008)

Magnetic measurements of  $\text{La}_{0.7}\text{Ca}_{0.3}\text{MnO}_3$  reveal a departure from Curie-Weiss behavior below the orthorhombic (O) to rhombohedral (R) structural transition at  $T_{O-R}=705$  K. Between  $T_{O-R}$  and  $T^*=273$  K, the magnetic response is clearly paramagnetic but with an enhanced magnetic moment attributed to the existence of small ferromagnetic polarons. These polarons grow in density and begin to interact below  $T^*$  as evidenced through low-field magnetic-susceptibility and field-dependent magnetization measurements, which show hysteresis and saturation, respectively. At the ferromagnetic transition temperature  $T_c=247.1$  K, the polarons coalesce and the system exhibits long-range ferromagnetism. It is asserted that the transition at  $T_c$  should be viewed as a polaronic to ferromagnetic phase transition. The relevance of the Griffiths phase is addressed.

DOI: [10.1103/PhysRevB.78.014436](https://doi.org/10.1103/PhysRevB.78.014436)

PACS number(s): 75.47.Lx, 71.38.-k, 75.40.Cx

Manganese oxides exhibiting colossal magnetoresistance (CMR) are complex magnetic conductors in which local lattice distortions, charge transport, and magnetic phenomenon are strongly intertwined.<sup>1</sup> One interpretation of the interesting behavior near and above the ferromagnetic transition temperature  $T_c$  focuses on ferromagnetic polarons (Ref. 2).  $\text{La}(\text{Ca})\text{MnO}_3$  near optimal doping exhibits local lattice distortions<sup>3,4</sup> in analogy to the electrostatic distortions associated with dielectric polarons.<sup>5,6</sup> Electrical transport is consistent with polarons,<sup>7</sup> and the lattice distortions along with the electrical conductivity are strongly influenced by magnetic field and temperature.<sup>3,4</sup> Neutron scattering reveals short-range ferromagnetic correlations attributed to ferromagnetic polarons whose number increases rapidly as  $T \rightarrow T_c$  from above;<sup>8,9</sup> a lack of divergence of the magnetic correlation length below  $T_c$  suggests a first-order ferromagnetic phase transition. However, thermodynamic measurements reveal a continuous (second-order) phase transition with an exceptionally large specific-heat exponent.<sup>10</sup> This dichotomy probably results from the order parameter being more complex than is the case for conventional ferromagnets,<sup>10,11</sup> where it is simply the magnetization.<sup>12</sup> Naturally, strong coupling<sup>1</sup> among charge, lattice, and magnetic degrees of freedom might lead to an order parameter involving all three.

A few years ago it was claimed that CMR is associated with the Griffiths phase.<sup>13</sup> True Griffiths behavior, because of its mathematical structure, is associated *only* with the Ising ferromagnet. It describes a diluted Ising ferromagnet with a transition temperature  $T_c < T_c(1)$ , where  $T_c(1)$  is the transition temperature associated with the undiluted Ising system.<sup>14</sup> In CMR systems, quenched disorder is argued to lead to a distribution of exchange energies that causes *Griffiths-like* behavior.<sup>13</sup> The Griffiths phase scenario is fundamentally different from a polaronic description of CMR materials. The present paper reports on magnetic-susceptibility ( $\chi$ ) measurements above  $T_c$  of  $\text{La}_{0.7}\text{Ca}_{0.3}\text{MnO}_3$ . The data reveal distinct features visible only at low magnetic field that can be qualitatively understood as the result of ferromagnetic polarons. The polarons display a range of be-

havior, depending on the temperature and field, that is clearly different above and below the temperature  $T^*=273$  K, which lies above  $T_c=247.1$  K. Above  $T^*$  the sea of ferromagnetic polarons is shown to be paramagnetic. Our reasoning for excluding the Griffiths phase scenario is based on theoretical principles as well as the scaling of  $\chi$  near  $T_c$ , which reveals strong magnetic-field dependence that was not previously considered.<sup>13</sup>

Polycrystalline  $\text{La}_{0.7}\text{Ca}_{0.3}\text{MnO}_3$  was prepared by a sol-gel method as described in detail previously.<sup>10</sup> Iodometric titration yielded the average Mn valence of 3.32(1). Magnetization  $M$  measurements were performed using a Quantum Design vibrating sample magnetometer (VSM). A long thin sample minimized demagnetization effects. Data were collected on cooling from 350 to 200 K, where the magnetic field  $H$  was oscillated to zero. Afterward, the sample was warmed to 350 K before applying field for the next measurement. In the range  $4.6 < H < 115$  Oe,  $H$  was determined by two procedures: measurement of  $\chi$  of Gd immediately after measuring the sample and use of the sample itself to probe  $H$ . In the latter, linearity of  $M(H)$  (above 300 K) was used to estimate the field. Absolute field magnitude and homogeneity for 0.2 and 1.5 Oe were determined with a fluxgate transformer; the 2-mm-amplitude VSM oscillation and inhomogeneity (0.03 Oe/cm) indicate a variation of 0.006 Oe during measurement at these fields. High-resolution thermal-expansion measurements utilized a fused-quartz capacitive cell.<sup>15</sup> Electrical resistivity was measured by the four-probe dc method.

Figure 1 displays  $\chi^{-1}$  corrected for the temperature-independent diamagnetic and Van Vleck contributions<sup>16</sup> between 10 and 900 K; these data reproduced on a second warming to 900 K. As  $T$  is increased, two features are observed: a ferromagnetic to paramagnetic phase transition at  $T_c=247.1$  K and a first-order structural transition from orthorhombic (O) to rhombohedral (R) at  $T_{O-R}=705$  K (note hysteresis in lower inset). The Curie-Weiss law, obeyed *only* above  $T_{O-R}$ , yields the effective magnetic moment  $p_{\text{eff}}=4.57(3)\mu_B$  (with Curie-Weiss temperature  $\theta=360$  K), where  $\mu_B$  is the Bohr magneton. This agrees with the ex-

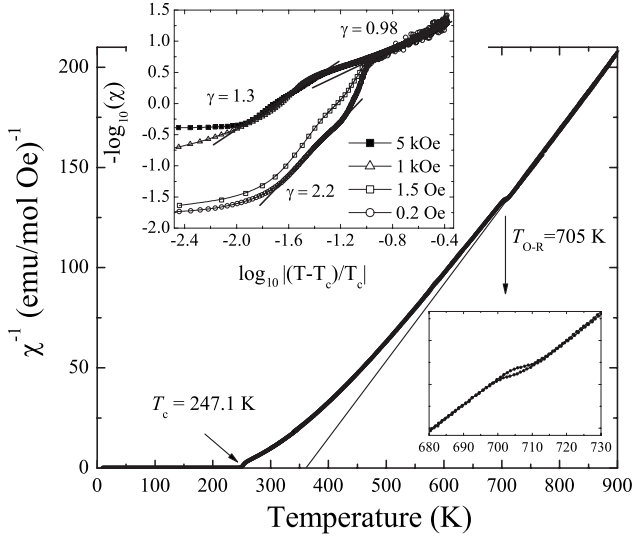


FIG. 1. Inverse magnetic susceptibility  $\chi^{-1}$  at  $H=1$  kOe. Lower inset shows the structural transition and hysteresis. Upper inset shows  $\chi$  on a log-log scale.

pected value ( $p_{\text{eff}}=4.59 \mu_B$ ) for spin-only Mn ions with the appropriate  $\text{Mn}^{4+}/\text{Mn}^{3+}$  ratio, suggesting minimal interaction among the magnetic ions in the R phase. Below  $T_{O-R}$  the slope of  $\chi^{-1}$  decreases monotonically as  $T_c$  is approached from above, suggesting the formation of short-range magnetic order. This behavior has been described using a mixture of free magnetic ions and pairs of Mn magnetic moments, coupled ferromagnetically via double exchange, whose population follows a Boltzmann distribution.<sup>17</sup> These ferromagnetic dimers behave as paramagnetic ions with enhanced moments.

Since  $\chi$  is defined<sup>18</sup> in the infinitesimal field limit [ $\chi=(\partial M/\partial H)_{H\rightarrow 0}$ ], we measured it in the lowest fields possible. Figure 2(a) shows  $\chi$  data along with the linear thermal-expansion coefficient ( $\mu$ ) measured in the earth's magnetic field (solid line exhibiting a peak). The  $\mu$  data clearly illustrate the bulk thermodynamic phase transition at  $T_c=247.1$  K. Focusing first on the 0.2 Oe data [the right-most curve in Fig. 2(a)], a significant increase in  $\chi$  is evident well above  $T_c$ . Similar behavior was reported previously in  $\text{La}_{2/3}\text{Ca}_{1/3}\text{MnO}_3$  and attributed to the formation of magnetic clusters.<sup>19</sup> With larger applied fields, this increase is pushed downward closer to  $T_c$ . This behavior is highlighted in the inset of Fig. 2(a) where the initial increase in  $\chi$  at  $T^*\approx 273$  K in  $H=0.2$  Oe is clearly visible; it is also evident in the  $\chi^{-1}$  data of Fig. 2(b). A very important aspect is that no signature of this feature is observed in our high-resolution thermal-expansion or heat-capacity (not shown) measurements, illustrating that it is *not* a bulk effect. Furthermore, significant hysteresis [inset of Fig. 2(b)] occurs in the region between  $T_c$  and  $T^*$ . We observed a similar downturn in  $\chi^{-1}$  above  $T_c$  in  $\text{La}_{0.75}\text{Sr}_{0.25}\text{MnO}_3$ . In addition, similar behavior is observed<sup>13,20</sup> in single crystals and  $\text{La}_{1-x}\text{Ba}_x\text{MnO}_3$ . Thus, this behavior is typical of CMR oxides.

Temperature hysteresis [inset of Fig. 2(b)] in  $\chi^{-1}$  reveals irreversibility in the region  $T_c < T < T^*$ , suggestive of magnetic frustration. We conducted extensive measurements of

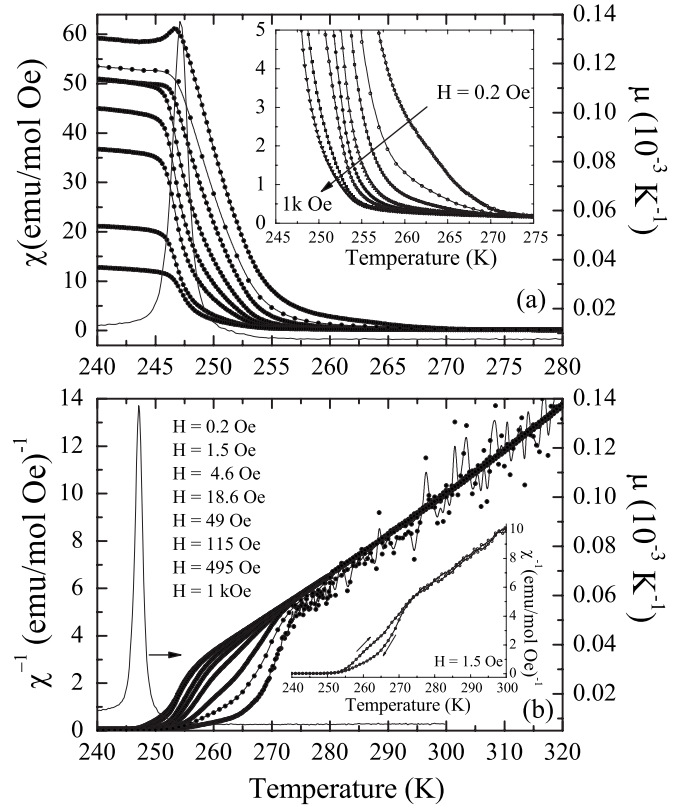


FIG. 2. (a) Magnetic susceptibility in several magnetic fields (highlighted in inset) and thermal-expansion coefficient  $\mu$  at zero field and (b)  $\chi^{-1}$  at the same fields. Inset shows hysteresis in  $\chi^{-1}$  at 1.5 Oe.

$M(H)$  above  $T^*$  to  $H$  as high as 80 kOe (see below). These data reveal  $M$  as linear in  $H$  (i.e., paramagnetic) below 18 kOe. Thus, even though formation of magnetic dimers<sup>4,17</sup> occurs above  $T^*$ , there is no evidence of saturation of  $M$  or the formation of magnetic domains in moderate magnetic field, which would signify the existence of long-range order. The  $M$  versus  $H$  data are discussed in detail below.

The Griffiths phase is claimed<sup>13</sup> to be identified by  $\chi^{-1}\propto(T-T_c)^{1-\lambda}$  with  $0<\lambda<1$ . Our evaluation of the published literature shows that the criterion  $0<\lambda<1$  does not serve to identify a Griffiths phase at all. In fact,  $\lambda<1$  is predicted only for the *quantum* Griffiths phase<sup>21</sup> ( $T_c=0$ ) in the special case of heavy-fermion materials. Here two further problems are revealed: the dependence of  $\lambda$  on  $H$  and the thermal history. The upper inset of Fig. 1 shows  $\chi$  versus  $(T-T_c)/T_c$  with ( $T_c=247.1$ ) on a log-log scale for  $H=0.2, 1.5, 1000,$  and  $5000$  Oe. Above  $T^*$  the exponent  $\gamma=1-\lambda=0.98$  is close to the value expected for a conventional paramagnet. In the region between  $T^*$  and  $T_c$ , the value  $\lambda=-1.2$  is obtained (at 0.2 Oe); note that the range of  $T$  where we extract  $\lambda$  is similar to the critical range in thermal-expansion data.<sup>10</sup> Measurement at  $H=1$  kOe (same field as used previously<sup>13</sup>) results in  $\lambda=-0.3$ . However, at this field the critical region is far narrower and a second linear region closer to  $T_c$  is apparent with  $\lambda=0.12$ , close to the reported value.<sup>13</sup> The strong-field effect on  $\lambda$  underscores the importance of measuring  $\chi$  at low field and the pronounced hys-

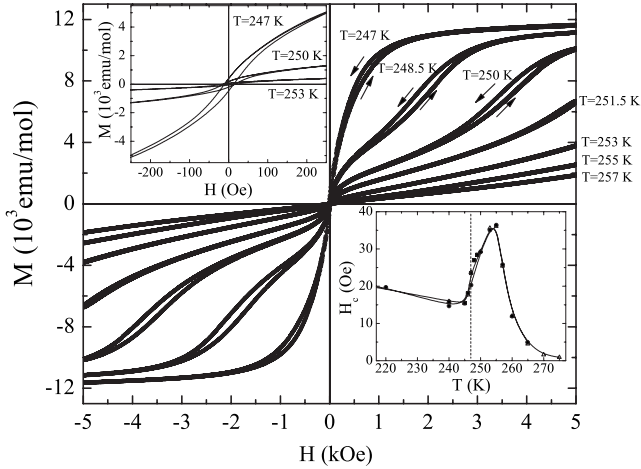


FIG. 3.  $M$  versus  $H$  loops for  $T$  near  $T_c$ . Upper inset shows similar data for  $|H| \leq 300$  Oe. Lower inset shows the coercive force  $H_c$  versus  $T$ ; vertical dashed line is at  $T_c$ .

teresis in  $T$  [inset of Fig. 2(b)] illustrates the importance of the measurement history.

Although Fig. 2 suggests that  $\chi$  measured on cooling is larger for smaller field near  $T_c$ , hysteresis in  $T$  [inset of Fig. 2(b)] and  $H$  must be considered. Figure 3 shows example of  $M(H)$  loops. There are a number of striking aspects of these data. Two distinct saturation plateaus are evident: one near 300 Oe (highlighted in upper inset of Fig. 3) and one at much higher field. This behavior is sometimes attributed to first-order nature<sup>22</sup> of the phase transition at  $T_c$ , but recent work shows that the transition is continuous (second order).<sup>10</sup> Focusing on the low-field plateau, hysteresis is evident. We determine the width of the hysteresis loops, the coercive force  $H_c$ , by measuring the spacing between the  $M(H)$  curves at  $M=0$  (plotted in the lower inset of Fig. 3).  $H_c=0$  above  $T^*$ , reaches a maximum immediately above  $T_c$  and decreases as  $T_c$  is approached.<sup>23</sup> The high-field plateau is also interesting. Using the data at 248.5 K as an example, there is hysteresis in the intermediate field range ( $800 < H < 2800$  Oe).

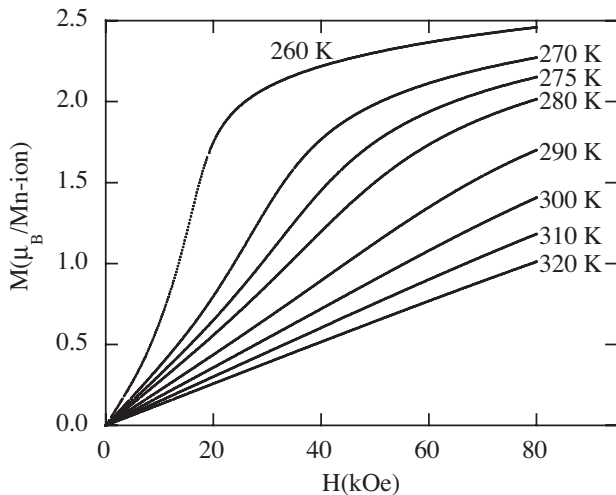


FIG. 4. Magnetization versus magnetic field above and below  $T^*$ .

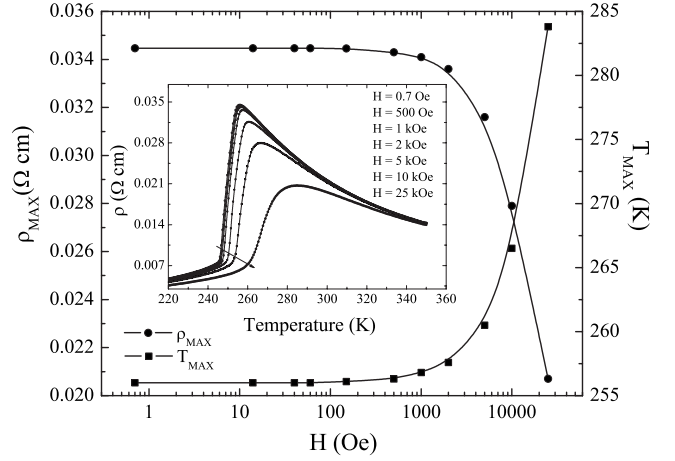


FIG. 5. Maximum value of the electrical resistivity  $\rho_{\text{MAX}}$  and its corresponding temperature  $T_{\text{MAX}}$  versus  $H$ . Inset shows  $\rho(T)$  in magnetic field.

Furthermore, the high-field saturation moves up strongly with an increased temperature at  $\approx 1300$  Oe/K. The high-field plateau remains evident to higher temperatures and fields as shown in Fig. 4.

The  $M$  versus  $H$  data in Fig. 4 illustrate the behavior of  $M$  for temperatures above and below  $T^*$  in higher magnetic field. It can be seen that as  $T^*$  is approached from above,  $M$  reveals only weak deviations from linearity for  $H < 80$  kOe at 320, 310, and 300 K. At 290 K a more distinct tendency to saturate appears near 60 kOe. This becomes significantly more pronounced for  $T < 290$  K, below which the  $M(H)$  data develop a high-field plateau similar to that observed in Fig. 3 at lower field. Immediately above  $T^*$  (see the curve at 275 K)  $M$  remains linear until 15 kOe, above which the slope  $dM/dH$  increases. This deviation from linearity, revealed as an increase in  $dM/dH$ , moves to higher field as the temperature is increased; it is no longer evident at 320 K for  $0 < H < 80$  kOe. The absence of hysteresis,  $H_c=0$ , and the linearity of  $M(H)$  suggest that above  $T^*$  the system is paramagnetic, as long as the applied field remains below approximately 18 kOe.

Despite large variations in  $\chi$  with  $H$  near  $T_c$ , the electrical resistivity  $\rho$  (Fig. 5) is barely influenced by fields below 2 kOe. Furthermore, it does not show hysteresis. These observations suggest that the regions of the sample responsible for electrical conduction are not influenced until the magnetic field reaches approximately 1000 Oe.

We now discuss the data. Below  $T_{O-R}=705$  K, the distinct deviation from Curie-Weiss behavior signals a competition between paramagnetism and the formation of ferromagnetic dimers. Presumably, orthorhombicity lowers the energy necessary for dimer formation. We believe that this is associated with the fact that the higher symmetry of the rhombohedral phase does not allow Jahn-Teller distortions,<sup>24</sup> which, upon formation, promote local ferromagnetic double exchange.<sup>17</sup> Since  $M(H)$  is linear, the ferromagnetic dimers<sup>4,17</sup> between  $T^*$  and  $T_{O-R}$  remain paramagnetic with regard to neighboring magnetic moments as long as the magnetic field is below about 18 kOe. We identify these as small ferromagnetic polarons,<sup>25</sup> of size comparable to the



pseudocubic lattice parameter  $a$ . Neutron diffraction reveals their growth in number<sup>2,8,9</sup> as the temperature is lowered, in agreement with the picture of Tanaka *et al.*<sup>17</sup> At  $T^*=273$  K, the distinct downturn in  $1/\chi$  [Fig. 2(b)] indicates significant growth in polaron size, probably a result of overlap; we hypothesize that these are large ferromagnetic polarons, of size larger than  $a$ . The  $M(H)$  data below  $T^*$  support this conjecture in that they reveal saturation and hysteresis, even in small magnetic fields. What we refer to as large polarons can also be thought of as regions of short-range order (SRO). SRO above  $T_c$  was predicted on a theoretical basis for some doping levels in the double-exchange model; the data in Fig. 2 clearly show a distinct transition above  $T_c$ , in support of this prediction.<sup>26</sup>

SRO coexisting with a paramagnetic background in the presence of strong charge, lattice, and spin coupling will be extremely frustrated. X-ray and neutron-diffraction studies of the polaron scattering<sup>9</sup> reveal a phase diagram including a region of temperature with dynamic polarons that, upon cooling, transform to a polaron glass phase just above  $T_c$ . This glassy state is likely to exhibit frustration, which is clearly evident in the hysteresis shown in the inset of Fig. 2(b). However, the diffraction data fail to reveal a distinct feature<sup>8,9,27</sup> at the temperature we refer to here as  $T^*$ .

The influence of magnetic field in the region  $T_c < T < T^*$  provides further insight; note that  $M(H)$  is linear above  $T^*$  (as long as  $H < 18$  kOe) and  $H_c = 0$ , suggesting paramagnetic behavior. We attribute the small saturation below 200 Oe (upper inset of Fig. 3) to rotation of the polarons in the direction of  $H$ ; the hysteresis signifies polaron-lattice coupling. At higher field, saturation of  $M$  is clearly evident. This saturation is attributed to growth of the polarons through overlap and their eventual formation into ferromagnetic domains. Hysteresis in this region of field is evident. According to the Néel theory<sup>28</sup> of coercive force, the energy associated with  $H_c$  in materials with large magnetostriction (as is the case with CMR materials)<sup>29</sup> is dominated by fluctuations in strain. With this in mind, the lower inset of Fig. 3 suggests that local strain associated with the large polarons maximizes just above  $T_c$  and decreases as the polarons coalesce at  $T_c$ , forming long-range ferromagnetic order. These observations are consistent with competition between thermal, magnetic (i.e.,  $\mu H$ , where  $\mu$  is the magnetic moment of a single Mn ion), and magnetic exchange energies among the paramagnetic Mn moments and magnetic polarons.

Hysteresis [inset of Fig. 2(b)] in  $\chi$  reflects a different magnetic evolution of polarons depending on whether the frustrated state is approached from above  $T^*$  (i.e., from the paramagnetic state) or below  $T_c$  (from the ferromagnetic state). In contrast, no hysteresis is observed in  $\rho(T, H)$  in the low-field region for  $T_c < T < T^*$ . This implies that the electrical resistivity is dominated by the paramagnetic regions. Within the polaron picture, on cooling below  $T^*$  in low field, newly formed large ferromagnetic polarons can become trapped with their moments restricted along a direction not parallel to the applied field. As magnetic field approaches 2 kOe, enough magnetic polarization of the polarons and intervening paramagnetic regions lead to percolative paths<sup>30</sup> through the polarons and a sizable decrease in  $\rho$ . As a result, the influence of small  $H$  on  $\rho$  should be minimal (as revealed in the resistivity data of Fig. 5).

Our discussion of the data in the upper inset of Fig. 1 reveals that  $0 < \lambda < 1$  is not satisfied. This condition on  $\lambda$  is often claimed to indicate the existence of a Griffiths phase.<sup>13,20</sup> Unfortunately, this is misleading. The condition  $\lambda < 1$  was determined<sup>21</sup> only for the specific case of heavy-fermion systems near  $T=0$ . This condition does not appear in any of the theoretical work on the Griffiths phase.<sup>14,31</sup>

The correctness of the Griffiths scenario for CMR systems is doubtful on a fundamental basis. The key to the existence of a Griffiths phase depends on the distribution of the partition function roots on the complex plane of the variable  $z = e^{-2\mu H/k_B T}$ , with  $H$  as a complex number. For an Ising ferromagnet, Lee and Yang<sup>32</sup> showed that the roots lie on the unit circle  $|z|=1$  for all temperatures. As the critical temperature is approached from above, at  $z=1$  the roots acquire nonzero density below  $T_c$ . At any  $T < T_c$ , the density of the roots is directly proportional to the magnetization. When randomly broken bonds exist, each connected not-yet-percolated cluster also respects the unit-circle theorem. With this in mind, the possibility exists that a site may belong to various possibly connected clusters with different probabilities. Griffiths showed that the magnetization as a function of  $z$  is not analytical at  $|z|=1$  for all  $T < T_c(1)$  with  $T_c(1)$  the critical temperature of the nondiluted Ising model.<sup>14</sup> For magnetic models other than Ising, the root distribution on the complex plane is unknown, as are the curves or trajectories on which the roots might be confined. Thus, the mathematical structure does not allow for the prediction of a Griffiths phase. In fact, the root distribution remains analytically unknown<sup>33</sup> for the antiferromagnetic Ising model. Some recent theoretical work<sup>34</sup> assumes the validity of the unit-circle theorem for other magnetic models for application to CMR, thereby deriving asymptotic behaviors for the magnetization near  $T_c$  and  $T_c(1)$ . This lack of mathematical rigor fails to add clarity to our understanding as the crux of the matter is to establish what gives rise to the unique behavior of CMR manganese oxides immediately above  $T_c$ . Furthermore, if the Griffiths scenario is correct for CMR systems, it must also lead to explanations for anomalous physical properties such as the huge negative magnetoresistance<sup>7</sup> and extremely large effect of pressure<sup>35</sup> on  $T_c$ .

To summarize,  $\chi(T)$  measurements at low magnetic field reveal physical characteristics unique to CMR manganese oxides. It is doubtful that this behavior can be attributed to a Griffiths phase. Our interpretation is that ferromagnetic polarons play a dominant role and that the behavior in the region between  $T_c$  and  $T^*$  results from frustrated ferromagnetic polarons. The existence and evolution of magnetic polarons over an extremely broad range of temperature ( $T_c < T < 705$  K) suggest that the phase transition at  $T_c$  should be designated a polaronic to ferromagnetic phase transition rather than a paramagnetic to ferromagnetic phase transition. This realization may eventually lead to an order parameter incorporating the strong interplay of charge, lattice, and magnetic degrees of freedom known to exist in CMR systems.

Thanks to Dr. Michael Simmonds and the staff at Quantum Design for their assistance and for the use of their flux-gate transformer. This material is based on work supported

by the Brazilian agency CNPq (Grant No. 201017/2005-9), the National Science Foundation (Grant No. DMR-0504769), the U.S. Department of Energy Office of Basic

Energy Sciences (Grant No. DE-FG-06ER46269), and the Intramural Research Program of the National Library of Medicine at the NIH.

\*Present address: Centro de Ciências Naturais e Humanas, Universidade Federal do ABC, 09090-900, Santo André, SP, Brazil.

- <sup>1</sup>E. Dagotto, T. Hotta, and A. Moreo, *Phys. Rep.* **344**, 1 (2001).
- <sup>2</sup>J. M. De Teresa, M. R. Ibarra, P. A. Algarabel, C. Ritter, C. Marquina, J. Blasco, J. García, A. del Moral, and Z. Arnold, *Nature (London)* **386**, 256 (1997).
- <sup>3</sup>C. H. Booth, F. Bridges, G. H. Kwei, J. M. Lawrence, A. L. Cornelius, and J. J. Neumeier, *Phys. Rev. Lett.* **80**, 853 (1998).
- <sup>4</sup>A. Daoud-Aladine, J. Rodríguez-Carvajal, L. Pinsard-Gaudart, M. T. Fernández-Díaz, and A. Revcolevschi, *Phys. Rev. Lett.* **89**, 097205 (2002); L. Downward, F. Bridges, S. Bushart, J. J. Neumeier, N. Dilley, and L. Zhou, *ibid.* **95**, 106401 (2005).
- <sup>5</sup>D. Emin, *Phys. Today* **35**(6), 34 (1982); **40**(1), 55 (1987).
- <sup>6</sup>R. P. Feynman, *Phys. Rev.* **97**, 660 (1955).
- <sup>7</sup>M. B. Salamon and M. Jaime, *Rev. Mod. Phys.* **73**, 583 (2001).
- <sup>8</sup>C. P. Adams, J. W. Lynn, Y. M. Mukovskii, A. A. Arsenov, and D. A. Shulyatev, *Phys. Rev. Lett.* **85**, 3954 (2000).
- <sup>9</sup>J. W. Lynn, D. N. Argyriou, Y. Ren, Y. Chen, Y. M. Mukovskii, and D. A. Shulyatev, *Phys. Rev. B* **76**, 014437 (2007).
- <sup>10</sup>J. A. Souza, Yi-Kuo Yu, J. J. Neumeier, H. Terashita, and R. F. Jardim, *Phys. Rev. Lett.* **94**, 207209 (2005).
- <sup>11</sup>J. A. Souza, J. J. Neumeier, B. D. White, H. Terashita, and Yi-Kuo Yu (unpublished).
- <sup>12</sup>K. Huang, *Statistical Mechanics* (Wiley, New York, 1987), p. 394.
- <sup>13</sup>M. B. Salamon, P. Lin, and S. H. Chun, *Phys. Rev. Lett.* **88**, 197203 (2002); M. B. Salamon and S. H. Chun, *Phys. Rev. B* **68**, 014411 (2003).
- <sup>14</sup>R. B. Griffiths, *Phys. Rev. Lett.* **23**, 17 (1969).
- <sup>15</sup>J. J. Neumeier, R. K. Bollinger, G. E. Timmins, C. R. Lane, R. D. Krogstad, and J. Macaluso, *Rev. Sci. Instrum.* **79**, 033903 (2008).
- <sup>16</sup>J. A. Souza, J. J. Neumeier, R. K. Bollinger, B. McGuire, C. A. M. dos Santos, and H. Terashita, *Phys. Rev. B* **76**, 024407 (2007).
- <sup>17</sup>J. Tanaka, H. Nozaki, S. Horiuchi, and M. Tsukioka, *J. Phys. (France) Lett.* **44**, L129 (1983).
- <sup>18</sup>M. E. Fisher, *Rep. Prog. Phys.* **30**, 615 (1967).
- <sup>19</sup>V. S. Amaral, J. P. Araújo, Y. G. Pogorelov, J. M. B. Lopes dos Santos, P. B. Tavares, A. A. C. S. Lourenço, J. B. Sousa, and J. M. Vieira, *J. Magn. Magn. Mater.* **226-230**, 837 (2001).
- <sup>20</sup>W. Jiang, X.-Z. Zhou, G. Williams, Y. Mukovskii, and K. Glazyrin, *Phys. Rev. Lett.* **99**, 177203 (2007); *Phys. Rev. B* **77**, 064424 (2008).
- <sup>21</sup>A. H. Castro Neto, G. Castilla, and B. A. Jones, *Phys. Rev. Lett.* **81**, 3531 (1998); A. H. Castro Neto (private communication).
- <sup>22</sup>J. Mira, J. Rivas, F. Rivadulla, C. Vázquez-Vázquez, and M. A. López-Quintela, *Phys. Rev. B* **60**, 2998 (1999).
- <sup>23</sup>Three  $H=0$  cooling modes were used prior to measuring  $M(H)$  to determine  $H_c$ : the sample was (1) warmed to 310 K and cooled at 20 K/min, (2) warmed to 310 K and cooled at 2 K/min, and (3) same as (2) with a 1 h wait prior to initiating the field sweep. Identical values for  $H_c$  were found (sweeps to maximum fields 300 Oe and 5 kOe).
- <sup>24</sup>J. Mira, J. Rivas, L. E. Hueso, F. Rivadulla, M. A. López Quintela, M. A. Señaris Rodríguez, and C. A. Ramos, *Phys. Rev. B* **65**, 024418 (2001).
- <sup>25</sup>D. Emin, M. S. Hillery, and Nai-Li H. Liu, *Phys. Rev. B* **35**, 641 (1987); D. Emin and M. S. Hillery, *ibid.* **37**, 4060 (1988).
- <sup>26</sup>R. S. Fishman, F. Popescu, G. Alvarez, T. Maier, and J. Moreno, *Phys. Rev. B* **73**, 140405(R) (2006).
- <sup>27</sup>J. W. Lynn (private communication).
- <sup>28</sup>R. M. Bozorth, *Ferromagnetism* (IEEE, New York, 1978), p. 827.
- <sup>29</sup>M. R. Ibarra, P. A. Algarabel, C. Marquina, J. Blasco, and J. García, *Phys. Rev. Lett.* **75**, 3541 (1995); J. J. Neumeier, A. L. Cornelius, M. F. Hundley, K. Andres, and K. J. McClellan, *Science and Technology of Magnetic Oxides*, MRS Symposia Proceedings No. 494 (Materials Research Society, Pittsburgh, 1998), p. 293.
- <sup>30</sup>L. P. Gor'kov and V. Z. Kresin, *J. Supercond.* **12**, 243 (1999).
- <sup>31</sup>A. J. Bray, *Phys. Rev. Lett.* **59**, 586 (1987); A. J. Bray and M. A. Moreo, *J. Phys. C* **15**, L765 (1982); A. J. Bray and D. Huifang, *Phys. Rev. B* **40**, 6980 (1989).
- <sup>32</sup>C. N. Yang and T. D. Lee, *Phys. Rev.* **87**, 404 (1952); T. D. Lee and C. N. Yang, *ibid.* **87**, 410 (1952).
- <sup>33</sup>X.-Z. Wang and J. S. Kim, *Phys. Rev. Lett.* **78**, 413 (1997).
- <sup>34</sup>P.-Y. Chan, N. Goldenfeld, and M. Salamon, *Phys. Rev. Lett.* **97**, 137201 (2006).
- <sup>35</sup>J. J. Neumeier, M. F. Hundley, J. D. Thompson, and R. H. Heffner, *Phys. Rev. B* **52**, R7006 (1995).